Thermochimica Acta, 238 (1994) 417–427
Elsevier Science B.V., Amsterdam
SSDI 0040-6031(93)01573-L

Thermophysical characterization of glassy, cross-linked heterocyclic polymers

V.P. Azarenkov, A.V. Baibak, V.Yu. Kramarenko and V.P. Privalko *
Institute of Macromolecular Chemistry, Academy of Sciences of Ukraine, 253160 Kiev (Ukraine)

(Received 27 January 1993; accepted 15 October 1993)

Abstract

An automated, computer-interfaced system was built and used for the characterization of the glassy state of a series of heterocyclic network polymers based on epoxy resin (ER) and hexamethylene diisocyanate (HMDI), using precise measurements of heat capacity and thermal conductivity in the temperature interval 80–315 K. The absolute values of both C_p and λ exhibit only moderate dependence on the network structure expressed by the HMDI/ER molar ratio. Moreover, no evidence for enthalpy relaxations in the range of temperatures studied is found from the heat capacity data for all samples, and in the intermediate temperature interval (120–220 K) the values of thermal conductivity for the sample with an HMDI/ER ratio of 80/20 passes through a shallow minimum which is tentatively attributed to the enthalpy-invariant motion of specific packing defects ("holes") in the glassy matrix.

INTRODUCTION

Densely cross-linked epoxies with excellent chemical resistance, and superior mechanical and thermal properties are widely used in many industrial applications [1–3]. So far, in studies of the structure–property relationships of such polymers, the main emphasis has been on their behavior around the glass transition interval [3–8], and considerably less attention has been paid to their properties at lower temperatures. In the present paper, we report on the measurements of heat capacity and thermal conductivity in the glassy state of a series of cross-linked polymers prepared by copolymerization of the base epoxy resin (ER) with different amounts of hexamethylene diisocyanate (HMDI).

* Corresponding author.

TABLE 1

Selected room-temperature properties of the samples studied

Property	HMDI/ER ratio		
	80/20	50/50	30/70
ρ/g cm^{-3}	1.240	1.210	1.205
T_g/K	390	343	331
E/GPa	1.52	1.83	2.02
B/GPa	6.80	4.77	3.22
V_T/km s^{-1}	0.64	0.72	0.77
V_L/km s^{-1}	2.40	2.14	1.85
M_c/g mol^{-1}	250	720	2100

EXPERIMENTAL

Materials

The cross-linked copolymers of ER and HMDI synthesized at 393 K for 2 h were essentially the same as those used in our previous studies [9–12]. Values of the glass transition temperature T_g, the room temperature density ρ, the bulk modulus B, Young's modulus E, the longitudinal V_L and transversal V_T sound velocity, and the mean molar mass of elastically active chain strands between the cross links M_c [11, 12], are collected in Table 1. Void-free specimens for thermal conductivity work were obtained by slow polymerization in evacuated, sealed ampoules.

Methods

The thermal conductivity λ was measured in steps of 5–7 K in the temperature interval 80–315 K using an absolute method of recording the longitudinal (axial) stationary heat flux [13] (Fig. 1). The upper and lower faces of a cylindrical sample, 6 (diameter 6 mm, height about 20–30 mm), are fixed to the upper block of the measuring device, 9, and to the sample heater, 7. The heater, 7, is thermally isolated from the lower block, 8.

Two radiation screens, 4 and 5, are fixed coaxially with the sample 6 to the upper and lower blocks by clamps, ensuring adequate thermal contact with the latter. Thus, thermal losses from the lateral surface of the sample are virtually eliminated.

Both the upper and lower blocks, as well as the sample heater, are made of polished, silver-coated copper. This ensures a minimal temperature gradient along the blocks and temperature stability during the transient period before the onset of the working regime.

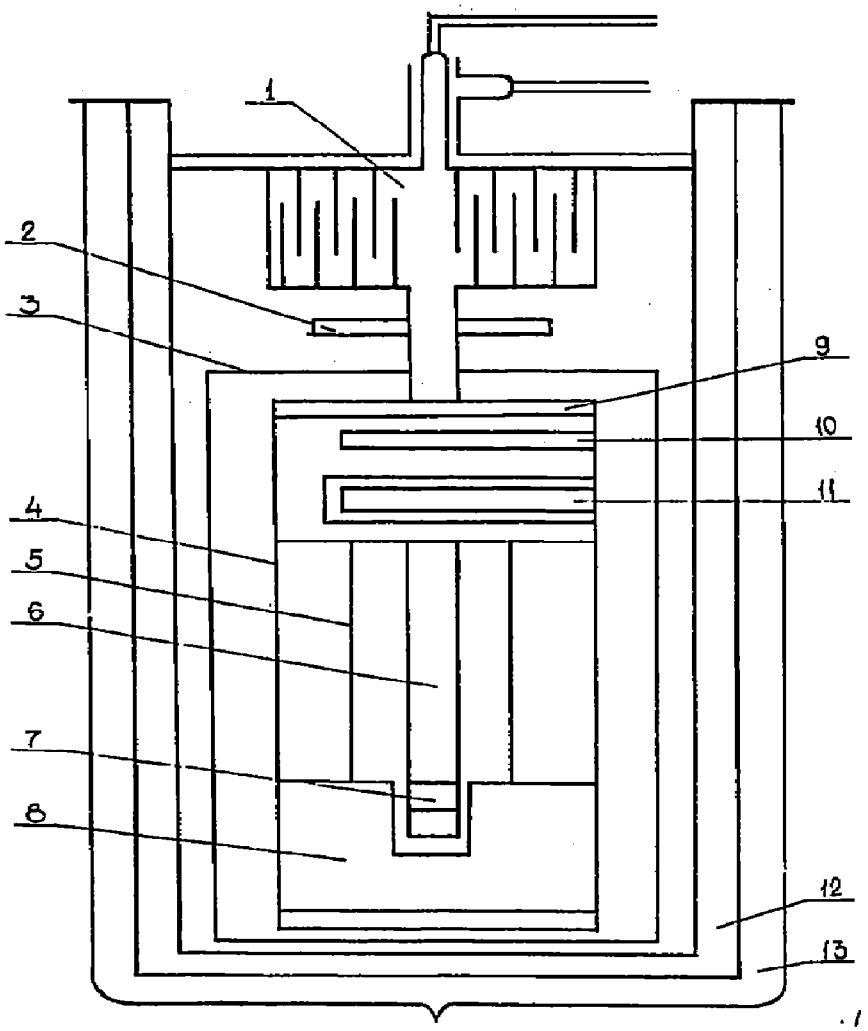

Fig. 1. Schematic of the unit for thermal conductivity measurements: 1, pipeline for the cooling agent supply; 2, background heater; 3, isolating shield; 4, 5, radiation screens; 6, sample; 7, sample heater; 8, lower block; 9, upper block; 10, monitoring thermocouple; 11, standard thermometer; 12, copper cup; 13, Dewar vessel.

Radiation screens made of 0.2-mm-thick, stainless-steel sheets, render both the deformation of the temperature field and the heat flow along the screens negligibly small. To minimize the heat losses by radiation from the latter, the measuring cell is surrounded by an isolating shield, 3, made of a polished, silver coated 0.3-mm-thick copper sheet.

Cooling agent, e.g. liquid nitrogen, is fed through the line 1 which allows control of the heat transfer from the cooling agent to the measuring cell by evacuating line 1 or by introduction of a heat transfer agent (helium). The background heater 2 which acts as a heat lock, i.e. it is switched on when

the deviation in the temperature of the cooling agent is above 50 K, is also located on-line between the heat exchanger and the measuring cell. The power supplied to the background heater is controlled to ensure the constancy of the power of the upper block heater up to the maximum temperature of the thermal conductivity measurements.

The sample temperature is measured with the aid of a standard thermometer, 11, and differential thermocouples, 10, one junction of which is fixed directly at the thermometer, 11, and the other directly onto the sample along the cell axis.

During the measurements, the temperature of the upper block is kept constant with the aid of a resistance thermometer, a heater and the channel of an automatic control system consisting of a nanovoltmeter R 341, a proportional-integral regulator R 111 and an input power amplifier. The temperature of the upper block, the temperature gradient along the sample ΔT, and the heat flux power W are recorded with the aid of an automatic measurements control system, and the relevant input data fed to the computer are converted into thermal conductivity values according to the relationship

$$\lambda = Wl/(\Delta TS)$$

where l is the sample length and S is the cross-sectional area of the sample.

The estimated mean error of the thermal conductivity measurements lies within the range of 3–4%.

The heat capacity C_p was measured with the aid of an adiabatic calorimeter integrated into the same computerized measurement system as described above (Fig. 2). The sample is placed into the container 3 (a cylindrical vessel 10 cm^3 in volume and 35 g in mass made of silver-coated copper with an upper cone-like neck) surrounded by a monitoring adiabatic shield, 6 (polished, silver coated copper vessel), ensuring minimal radiation heat transfer. Eight junctions of a copper–constantan thermopile are glued to the surfaces of both container 3 and shield 6. The thermopile is connected to the circuit of an automatic control system (ACS) and the heater of the shield, the temperature of the latter being kept equal to that of the container to within 5×10^{-5} K (at liquid helium temperature) or about 10^{-3} K (at around room temperature) to ensure the adiabatic measurement regime. All connecting wires of both container and adiabatic shield are connected to the "hot", i.e. heated, ring with the temperature being kept equal to that of the shield by use of a two-junction thermocouple and a channel of the ACS. Both the adiabatic shield and the hot ring are surrounded by the equilibration shield 5 which has an in-built heater. The two-junction thermocouple placed between the equilibration shield and the hot ring is connected to the channel 13-11-12, provided with the circuit of the thermocouple current shift. The latter is used to keep the temperature

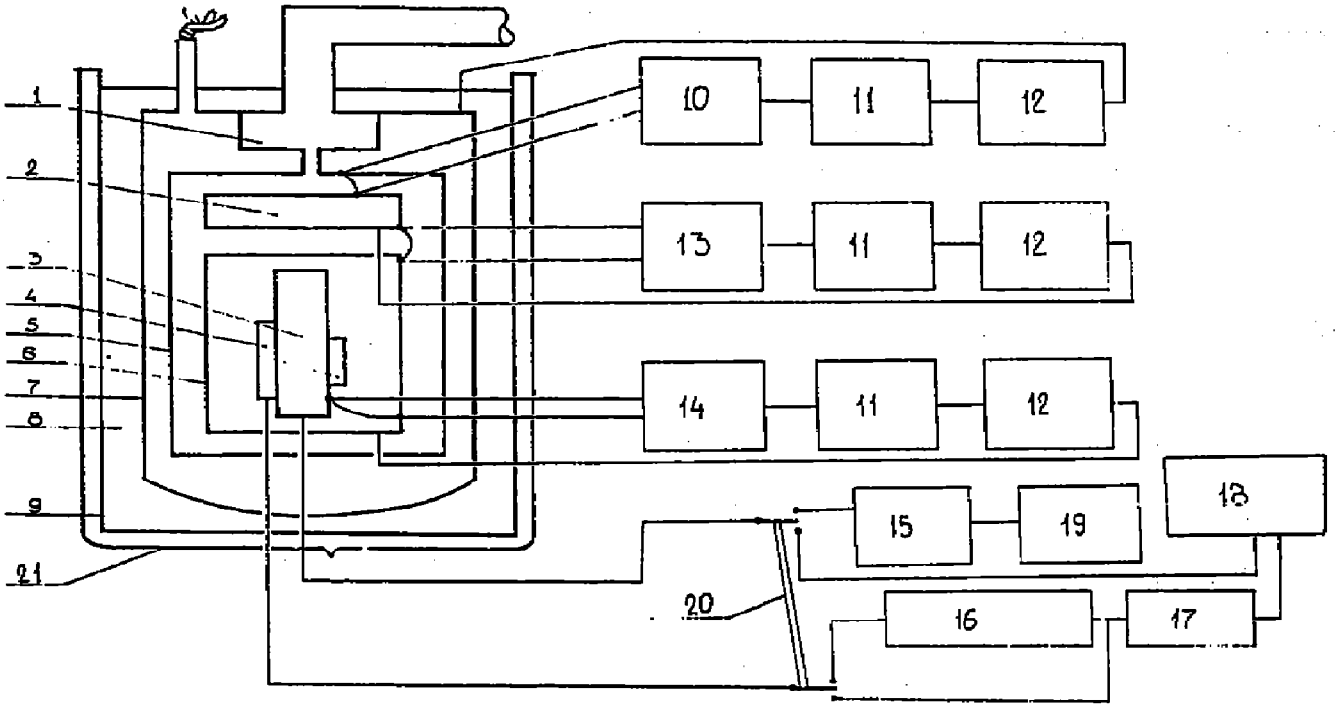

Fig. 2. Schematic of the unit for heat capacity measurements: 1, "cold" ring; 2, "hot" ring; 3, sample container; 4, recording thermometer; 5, equilibration shield; 6, monitoring adiabatic shield; 7, copper cup; 8, cooling agent; 9, Dewar vessel; 10, 11, 12; 13, 11, 12; 14, 11, 12, channels of the temperature monitoring and control system; 15, 19, channel of heater current control; 16, 17, recording channel ; 18, computer; 20, switch for the change in working mode (automatic/manual).

of the equilibration shield somewhat below that of the adiabatic shield in order to control the temperature regimes of the ring and of the adiabatic shield. To eliminate heat losses, all connecting wires coming from the room temperature environment are glued to the "cold" ring.

The whole calorimetric unit is placed inside the housing 7, tightly connected to the vacuum system. Thus, the main source of possible heat losses, i.e. convection currents, is eliminated by evacuation of the calorimeter to about 10^{-6} Torr at liquid helium temperature and to 5×10^{-5} Torr at higher temperatures.

The ACS channels providing adiabatic conditions are comprised of pre-amplifiers F 136 and R 341, temperature regulators R 111 and power amplifiers. The temperature of the sample container is measured with resistance thermoconvertors TS-MF-D (in the temperature interval below 10 K) and platinum resistance thermometers (at higher temperatures) placed in copper ampoules on the container surface. The data on the resistance of the thermometers and the power supply to the container heater are converted into container temperature and the quantity of heat ΔQ, respectively, with the aid of a digital voltmeter SHCH 31 and a

comparator R 3003 switched in the compensation mode. The time spent on the step-like heat supply into the calorimetric unit is monitored with the aid of an electronic timer STTS-1.

The general routine for heat capacity measurements consists of the following stages. After adiabatic conditions at the desired temperature are established, the temperature increment of the calorimeter is shortened to ensure its linearity (usually in the limits of 10^{-4} to 10^{-3} K min^{-1}), the heat supply is switched on at the time t_1, and switched off after the time interval Δt, i.e. at the next moment t_2 $(=t_1 + \Delta t)$, and the temperature run is shortened once again to ensure its linearity. The starting and final temperatures of the calorimeter, T_1 and T_2, are obtained by extrapolation of both runs to the midpoint of the heating cycle, and the mean heat capacity of the loaded container in the temperature interval $\Delta T = T_2 - T_1$ is calculated as

$$\sum C_p = \Delta Q / \Delta T$$

where $\Delta Q = JV\,\Delta t$ is the quantity of heat supplied, and J and V are the current and voltage of the heater. The specific heat capacity of the sample of mass m is finally obtained as

$$c_p = \left(\sum C_p - C_{p,0}\right)/m$$

where $C_{p,0}$ is the heat capacity of the empty container (calibration constant).

The value of C_p found in this fashion refers to the mean temperature within the selected interval, $T = (T_1 + T_2)/2$. Given the standard widths of the temperature intervals, $\Delta T = 0.1$–0.5 K (around the liquid helium temperature) and $\Delta T = 3$–5 K (at higher temperatures), this mean heat capacity is believed to be identical to the true heat capacity of the studied substance (at least, in the temperature intervals of its smooth variation located sufficiently far from the phase transition regions). Control experiments with standard substances (corundum and benzoic acid) have shown the mean error of the heat capacity determination with our technique to be about 2% in the interval 4.2–80 K, 1% in the interval 80–150 K, and 0.5% in the interval 150–315 K.

RESULTS AND DISCUSSION

Because the raw values of the heat capacity of all samples varied smoothly with temperature without any evidence for the occurrence of enthalpy relaxation over the entire interval of the measurements, 80–315 K, these data were computer-fitted to n-power polynomials. It turned out that the experimental data were reproduced to within the experimental

TABLE 2

Smoothed values of the specific heat capacity in J kg^{-1} K^{-1} [a]

T/K	HMDI/ER ratio			T/K	HMDI/ER ratio		
	80/20	50/50	30/70		80/20	50/50	30/70
80	356.80	382.42	358.73	190	834.29	834.49	800.40
90	413.33	422.28	399.59	200	876.93	877.50	841.42
100	456.83	462.44	440.01	210	920.17	921.05	882.80
110	499.69	502.86	480.10	220	964.12	965.23	924.51
120	542.03	543.49	519.98	230	1008.92	1010.09	966.53
130	584.00	584.32	559.75	240	1053.45	1055.69	1008.78
140	625.65	625.35	599.48	250	1101.53	1102.05	1051.17
150	667.18	666.59	639.27	260	1149.60	1149.19	1093.53
160	708.68	708.08	679.20	280	1249.85	1245.69	1177.32
170	750.29	749.85	719.33	300	1356.44	1344.50	1257.72
180	792.11	791.97	759.71				

[a] The last non-significant digit in the c_p values has been included to avoid introduction of deviations through arithmetical causes.

uncertainty with any n chosen from 2 to 6. The smoothed values obtained setting $n = 6$ are presented in Table 2. It can also be readily verified that the double logarithmic heat capacity versus temperature plots are, to a very good approximation, linear, i.e. the following empirical relationship applies

$$C_p \approx T^{\alpha} \tag{1}$$

with the values of α shown in Table 3.

The theoretical significance of the values of α obtained for our amorphous, i.e. glassy, samples is difficult to assess, although they are fairly close to those obtained by Hartwig [14] for other cross-linked epoxies in a similar temperature interval. In qualitative terms, the situation may be visualized as follows.

In general, the proportionality eqn. (1) with $\alpha \approx 1$ should hold [15] if the

TABLE 3

Values of the parameters of eqns (1) and (4) for different HMDI/ER ratios

Parameter	HMDI/ER ratio		
	80/20	50/50	30/70
α	0.98	0.96	0.95
β	1.20	–	0.55

experimental temperature interval lies sufficiently lower than the relevant characteristic temperature of the acoustical vibrations θ, because in that case the vibration density of states $D(\omega)$ would obey the power law

$$D(\omega) \approx \omega^{n-1} \approx \text{constant} \tag{2}$$

where ω is the frequency of the acoustical vibrations. It is obvious, however, that the constancy of $D(\omega)$ may only be expected at extremely low temperatures ($T \ll \theta$) where the wavelength of the vibrations is extremely large [15, 16], whereas the temperature interval of our measurements corresponds, approximately, to a vibration wavelength of the order of fractions of a nanometer [17].

However, in the latter range of "high" temperatures where contributions from longitudinal and transversal, i.e. bending, acoustical vibrations manifest themselves as linear and square root-terms, respectively, in the equation [17, 18]

$$C_p \approx \text{const}_1\ T + \text{const}_2\ T^{1/2} \tag{3}$$

a power law, eqn. (1) with $\alpha \approx 1$, may also be observed provided the first term dominates. Apparently, this is consistent with our data.

The experimental values of the thermal conductivity of the sample HMDI/ER = 30/70 initially increase smoothly with temperature, without appreciable scatter, to an apparent plateau in the interval 180–230 K. Then, after a further slight increase, they finally level off above 270 K. Least-squares analysis has shown that these data fitted to within 1% to a single six-power polynomial. However, the raw values of λ for the HMDI-rich sample HMDI/ER = 80/20, after an initial rather steep rise in the interval 80–120 K, pass through a shallow minimum around 170 K, rise again, and then tend to level off above 250 K. In other words, both the absolute values of λ as well as the pattern of corresponding temperature dependences for samples with different HMDI/ER ratios are essentially similar in the temperature intervals below 120 K and above 220 K, respectively, whereas at intermediate temperatures the values of λ for the sample HMDI/ER = 80/20 are about 10–12% lower. Repeated upward and downward, i.e. heating and cooling, runs in the temperature interval 120–200 K confirmed the reproducibility of the experimental values of λ for the latter sample. In this case, two polynomials had to be used for a quantitative representation of the data, namely, a six-power polynomial for the temperature interval 80–210 K, and two-power polynomial for higher temperatures. The smoothed values of λ for these two samples (Table 4) are plotted versus temperature in Fig. 3, and the exponents in the power law equation

$$\lambda \approx T^{\beta} \tag{4}$$

valid for the limited temperature intervals (80–100 K and 80–130 K for

TABLE 4

Smoothed values of thermal conductivity/W m $^{-1}$ K $^{-1}$

T/K	HMDI/ER ratio		T/K	HMDI/ER ratio	
	80/20	30/70		80/20	30/70
80	0.173	0.189	200	0.243	0.266
90	0.201	0.201	210	0.255	0.267
100	0.222	0.213	220	0.258	0.267
110	0.235	0.225	230	0.260	0.268
120	0.240	0.235	240	0.262	0.269
130	0.241	0.243	250	0.264	0.271
140	0.239	0.250	260	0.265	0.272
150	0.236	0.255	270	0.266	0.274
160	0.234	0.259	280	0.267	0.275
170	0.232	0.262	290	0.267	0.276
180	0.232	0.264	300	0.268	0.276
190	0.235	0.265	310	0.268	0.276

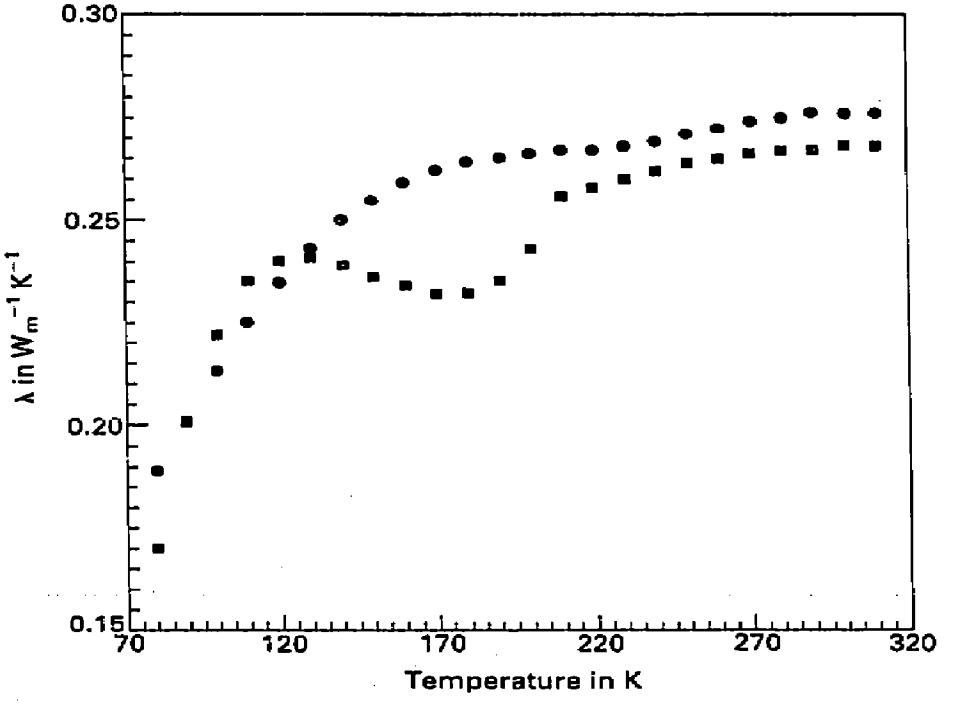

Fig. 3. Thermal conductivities of samples HMDI/ER = 80/20 (■) and HMDI/ER = 30/70 (●).

samples HMDI/ER = 80/20 and HMDI/ER = 30/70, respectively) are also shown in Table 3.

As can be seen from the tables, the room-temperature values of the specific heat capacity c_p, the density ρ, and the longitudinal sound velocity V_L for the sample HMDI/ER = 30/70 are lower compared to those of the sample HMDI/ER = 80/20, while the reverse is true for the transversal sound velocity V_T and thermal conductivity λ. In terms of the familiar equation

$$\lambda = C_V \langle V \rangle \langle l \rangle \rho / 3 \tag{5}$$

where $\langle V \rangle = (V_L^{-3} + 2V_T^{-3})^{-1/3}$ is the mean velocity of propagation of phonons in isotropic solids, $\langle l \rangle$ is the corresponding mean free path, and C_V is the isochoric heat capacity which is usually negligibly different from the experimental, isobaric C_p for solids, all these data may be rationalized assuming $\langle l \rangle \approx 0.9$ nm for both samples. It is difficult at the present stage to assign an unequivocal physical significance to the value of $\langle l \rangle$ derived in this fashion, although it is of the same order of magnitude as the lower structural limit of the fractal-like behavior of these samples [12] or the characteristic linear dimension of the model, anharmonic quasi-oscillator [11] (in Frenkel's sense [19]).

Unfortunately, little can be said about the possible origin of the difference between thermal conductivities of the samples in the temperature interval 120–220 K (Fig. 3). Qualitatively, similar patterns of the specific heat capacity behavior (Table 2), together with the difference between those for λ, imply different responses to temperature of those parameters of eqn. (5) which are sensitive to the defect state of the sample, i.e. $\langle V \rangle$ and ρ. Thus, one may speculate about a specific kind of defect motion in the glassy matrix of HMDI/ER = 80/20, e.g. a local, non-cooperative process of redistribution of "holes", which would not involve an appreciable enthalpy change. Clearly, more detailed acoustical measurements are needed to shed some light on this problem.

CONCLUSIONS

The automated, computer-interfaced system described in this paper was used to characterize the glassy state properties of a series of heterocyclic polymer networks based on epoxy resin (ER) and hexamethylene diisocyanate (HMDI) by precise measurements of heat capacity and thermal conductivity in the temperature interval 80–315 K. The absolute values of both C_p and λ exhibit only moderate dependence on the network structure expressed by the HMDI/ER molar ratio. Moreover, no evidence for enthalpy relaxations in the range of temperatures studied is found from heat capacity data for all samples, while in the intermediate temperature interval (120–220 K) the thermal conductivity values of the sample

HMDI/ER = 80/20 passes through a shallow minimum which is tentatively attributed to the enthalpy-invariant motion of specific packing defects ("holes") in the glassy matrix.

REFERENCES

1 V.I. Irzhak, B.A. Rosenberg and N.S. Enikolopyan, Network Polymers. Synthesis, Structure, Properties, Khimia, Moscow, 1979, pp. 627 (in Russian).
2 N. Kinjo, M. Ogata, K. Nishi and A. Kaneda, Adv. Polym. Sci., 88 (1989) 1.
3 B. Fuller, J.T. Gotro and G.C. Martin, Adv. Chem. Ser. No. 227, (1990) 215.
4 G.C. Stevens and M.J. Richardsom, Polymer, 24 (1983) 851.
5 V. Bellenger, E. Morel and J. Verdu, J. Mater. Sci., 23 (1988) 4244.
6 G. Wisanrakkit and J.K. Gillham, J. Coat. Technol., 62 (1990) 35.
7 J.P. Pascault and R.J.J. Williams, J. Polym. Sci. Polym. Phys. Ed., 28 (1990) 85.
8 A. Hale, C.W. Macosko and H.E. Bair, Macromolecules, 24 (1991) 2610.
9 V.P. Privalko, V.Yu. Kramarenko and A.M. Feinleib, Makromol. Chem., Macromol. Symp., 44 (1991) 247.
10 V.P. Privalko and V.Yu. Kramarenko, Polymer Sci. USSR, 34 (1992) 265.
11 V.P. Privalko, V.Yu. Kramarenko, Yu. V. Maslak and V.F. Rosovitsky, Colloid Polym. Sci., in press.
12 V.N. Novikov, A.P. Shebanin, V.P. Azarenkov, A.V. Baibak, V.Yu. Kramarenko and V.P. Privalko, J. Raman Spectrosc., submitted.
13 V.P. Azarenkov, A.V. Baibak and V.P. Privalko, in preparation.
14 G. Hartwig, Progr. Colloid Polym. Sci., 64 (1978) 56.
15 S. Hunklinger and A.K Rauchaudhuri, in D. Brewer (Ed.), Progress in Low Temperature Physics Vol. 9, Elsevier, Amsterdam, 1986, p. 267.
16 C.J. Nichols and H.M. Rosenberg, J. Phys. C, 17 (1984) 1165.
17 G. Hartwig, Habilitationsarbeit, Univ. Erlangen, 1989.
18 S.M. Genensky and G.F. Newell, J. Chem. Phys., 26 (1957) 486.
19 Ya.I. Frenkel, Introduction to the Theory of Metals, Gosizdattekhlit, Moscow, 1948 (in Russian).